

Fabrication of chitosan-based electrospun nanofiber scaffold: Amplification of biomechanical properties, structural stability, and seeded cell viability

Mohammad Mahdian-Dehkordi¹, Farshid Sarrafzadeh-Rezaei^{1*}, Mazdak Razi², Mehdi Mahmoudian³

¹ Department of Surgery and Diagnostic Imaging, Faculty of Veterinary Medicine, Urmia University, Urmia, Iran; ² Department of Basic Sciences, Faculty of Veterinary Medicine, Urmia University, Urmia, Iran; ³ Nanotechnology Research Center, Urmia University, Urmia, Iran.

Article Info

Article history:

Received: 14 March 2020
Accepted: 01 June 2020
Available online: 15 March 2021

Keywords:

Biomaterial
Borax
Cell seeding
Cross-linking
Electrospinning

Abstract

The cell scaffolds should structurally be manufactured similar to the target tissue's extracellular matrix. This property should be maintained until cell differentiation. For this purpose, in the current study, electrospun nanofiber (EN) of chitosan (Ch)/polyvinyl alcohol (PVA), as a tissue-friendly scaffold, was fabricated by electrospinning in different formulations and borax was utilized as an innovative cross-linking agent to up-regulate the structural and biomechanical properties. The weight loss, water absorbability, structural stability, tensile strength and biocompatibility of borax-included and non-included ENs were compared. The finest morphology, weight loss, water absorbability, structural stability in an aqueous environment, tensile strength and cell viability were found in the borax-included EN containing Ch50.00%v/PVA50.00%v. Moreover, The ENs exhibited appropriate antibacterial properties against Gram-positive and Gram-negative bacteria. In conclusion, borax can be used to improve the mechanical and biocompatibility features of the Ch/PVA-based ENs. Furthermore, it could be suggested that borax-included Ch/PVA ENs can exhibit high appropriate biological properties, candidate them as an appropriate scaffold in the field of tissue engineering. However, *in vivo* trials are needed to clearly their side effects and advantages.

© 2021 Urmia University. All rights reserved.

Introduction

Tissue engineering is an interdisciplinary science in which the scaffolds, cells, and growth factors improve and accelerate the healing process in different tissues.¹ Although tissue engineering is known as a treatment-friendly and attractive method, selecting an appropriate scaffold for specialized tissue or case needs more attention due to physicochemical and structural features.²⁻⁴ Based on this fact, several studies have been conducted to promote the scaffold's structural, biochemical and mechanical characteristics.⁵⁻⁹ Indeed, the main reason for using scaffold in tissue engineering is to mimic the native/physiological extracellular matrix (ECM) of tissues. Considering that the scaffolds are temporary structures, biocompatibility, biodegradability, safety (to be non-toxic), and structural integrity are necessary until natural ECM replacement during the wound healing process.¹⁰

Chitosan (Ch), a cationic linear natural polysaccharide, is utilized in nanofibrous scaffold fabrication due to appropriate biological features.¹¹⁻¹³ The Ch-based nanofiber is widely used as a scaffold for tissue engineering purposes, including skin, bone, cartilage, nerve, and vascular tissue engineering.^{9,14-17} In this line, the nanofiber-based scaffolds, fabricated by electrospinning, topographically exhibit various features, including a high surface area to volume, porosity, and three-dimensional network, all are making them ideal candidates as scaffolds in tissue engineering.¹⁸ The electrospinning is the most common method for nanofibers fabrication due to cost-effectiveness, easy usage, scalability, repeatability, and ability to produce long-length nanofibers.¹⁹ The Ch does not provide sufficient necessary mechanical properties in nanofibers production using electrospinning. Thus, it is usually combined with other polymers in the electrospinning process. In agreement with this issue, various polymers such as hydroxyapatite, polyethylene oxide and

*Correspondence:

Farshid Sarrafzadeh-Rezaei. DVM, DVSc
Department of Surgery and Diagnostic Imaging, Faculty of Veterinary Medicine, Urmia University, Urmia, Iran
E-mail: f.sarrafzadeh@urmia.ac.ir



This work is licensed under a Creative Commons Attribution-NonCommercial 4.0 International License which allows users to read, copy, distribute and make derivative works for non-commercial purposes from the material, as long as the author of the original work is cited properly.

gelatin are used to blend with Ch during electrospinning to prepare appropriate nanofibers.^{6,8,9,20,21} Among different blending polymers, polyvinyl alcohol (PVA), a water-soluble synthetic polymer, is included in the electrospinning process as a co-blending polymer with Ch.²²

Although biodegradable polymers are used in Ch-based scaffolds fabrication, they are not solely appropriate because of low resistance in the aqueous environment and weak mechanical strength after nanofabrication. Accordingly, nanofibers' resistance in aqueous environments such as various live tissues has improved by enhancing the cross-link between fibers. For this purpose, multiple chemicals such as genipin, glutaraldehyde vapor, and poly (ethylene glycol) diacrylate are used and reported by different researchers.²³⁻²⁵ However, most of these compounds have shown to adversely affect the biological systems or seeded cells when they are included at high levels. Moreover, long-time processing for fabrication is known as another disadvantage for the materials, as mentioned earlier. Therefore, considering the importance of cross-linking in the structure of electrospun nanofibers (ENs) and in line with this issue, borax has recently gained more attention. Accordingly, borax was successfully used as a cross-linking agent in an Arabic gum, gelatin scaffold,²⁶ starch-PVA film²⁷ and gelatin hydrogel.²⁸ Although borax has been successfully used in the above-named materials, it is not considered in nanofiber-based scaffolds. Thus, in the current study, borax was included in ENs for the first time and different methodologies were used to evaluate its possible promoting impact on ENs.

Based on this concept, this study aimed to fabricate scaffold being structurally and biologically appropriate/applicable in the wound healing process and tissue engineering.

Materials and Methods

Chemicals. Low molecular weight Ch with 75.00% deacetylation (Sigma-Aldrich, Munich, Germany), PVA (Mw: 72,000 g mol⁻¹, hydrolysis ≥ 98.00%), di-sodium tetraborate (Borax), 100% acetic acid (glacial), and absolute ethanol (Merck, Darmstadt, Germany) without purification were used in this study. Fibroblast cell line (NCBI code: c147) was purchased from Pasteur Institute of Iran (Tehran, Iran), and culture media (RPMI 1640 and FBS; Thermo Fisher Scientific, Waltham, USA) were obtained from Bioidea Company (Tehran, Iran). The MTT assay kit from DNAbiotech Co. (Tehran, Iran) was also used.

Preparation of electrospinning solutions. The aqueous solutions of Ch (2.00% wt) and PVA (10.00% wt) were prepared separately. A 0.50 M solutions of acetic acid and distilled water were used as solvents. The solutions were mixed in different concentrations: Ch30.00%/PVA70.00%: Ch/PVA1, Ch40.00%/PVA60.00%: Ch/PVA2,

Ch50.00%/PVA50.00%: Ch/PVA3, Ch60.00%/PVA40.00%: Ch/PVA4 and Ch70.00%/PVA30.00%: Ch/PVA5. The mixed solutions were centrifuged and stored overnight to remove the air bubbles.

Electrospinning conditions. Electrospinning was carried out using a 5.00 mL syringe and needle with an internal diameter of 0.514 mm. An aluminum foil-coated rotary plate was used as a collector. The distance between the collector and needle was about 10.00 cm, and the supplementary voltage was set at 20.00 kV. Rotation speed was regulated at 50 rpm, and the injection rate was 8.00 μL per min. The ENs were spun in about 48 hr. Finally, the prepared ENs were separated from foil and dried in a vacuum oven at 50.00 °C.

Cross-linking of ENs. For induction of a cross-linking reaction in the ENs, a mixture of borax in ethanol (1.00% wt) was prepared. The fabricated ENs were immersed in the borax solution, maintained for 10 min at room temperature, washed several times with ethanol, and dried samples were obtained after the vacuum drying process. The borax-included ENs were marked with the letter B.

Field emission scanning electron microscopy (FESEM). The FESEM (Nova NanoSEM 450; FEI Co., Hillsboro, USA) was used to analyze the morphology of ENs. The average diameter of fibers was evaluated on FESEM images using Digimizer software (version v5.3.5; MedCalc Software Ltd., Ostend, Belgium). Accordingly, the diameter of 30 fibers was measured randomly.

Weight loss, water absorbability, and structural stability in the aqueous environment determinations. To determine the weight loss, the ENs were placed into phosphate-buffered saline (PBS; pH 7.40) solution at room temperature. Weight loss test was performed by immersing the exact weight of ENs (1.50 cm²) in a buffer solution, removing from buffer solution, and weighing after drying in a vacuum oven. The weight loss was calculated based on the initial dry weight (W_i) and final dry weight (W_f) using the equation (1). Water absorbability was calculated (according to equation (2)) similar to the weight loss test, except that the ENs were weighted after removing the surface water with filter paper (W_s). For each sample, three replicates were considered.²⁹ Moreover, to evaluate the structural stability in an aqueous environment, the ENs were placed in a PBS, and after 1, 3, and 7 days, the ENs were dissected out, dried, and processed for FESEM.³⁰

$$(1) \text{ Weight loss (\%)} = [(W_i - W_f) / W_i] \times 100$$

$$(2) \text{ Water absorbability (\%)} = [(W_s - W_i) / W_i] \times 100$$

Tensile strength. The ENs were cut into dumbbell shapes with a specific size (1.00 × 5.00 cm) and stored in constant conditions for 24 hr. To evaluating the tensile strength, the texture analyzer machine (TA-XT plus; Stable Micro Systems, Godalming, UK) was used with a load cell

of 5.00 N and a velocity of 10 mm per min. The average values of three experiments for each sample were obtained and compared.³¹

Antibacterial property test. *Escherichia coli* (ATCC 25922), *Staphylococcus aureus* (ATCC 25923), and *Pseudomonas aeruginosa* (ATCC 27853) were obtained from Persian Type Culture Collection (Tehran, Iran). According to the guidelines of the Clinical and Laboratory Standards Institute, the antibacterial activities of ENs against the mentioned strains were evaluated using the parallel streak method (AATCC 147). For this purpose, the bacteria were cultured aerobically in tryptic soy broth (TSB; Laboratories CONDA, Madrid, Spain) at 37.00 °C for 18 hr. The culture solution was diluted with TSB (6×10^7 CFU mL⁻¹) by a turbid metric method at 550 nm wavelengths using a UV-spectrophotometer (UNICO, Shanghai, China). Plate count agar (PCA) and 2-3-5-triphenyl-2H-tetrazolium chloride (Laboratories CONDA, Madrid, Spain) were autoclaved and poured into 60.00 mm diameter Petri dishes. One loopful of bacterial dilution was streaked on the PCA in five parallel lines. The ENs were cut into 2.50 × 5.00 cm pieces and placed transversely across the five lines streaked previously on the plates. Plates were incubated at 37.00 °C for 24 hr, and interruption of the growth line under the mats was evaluated. For the control group, sterile cotton gauze was placed on the agar, exactly like mats.³²

Cell culture, cell seeding, and MTT assay. Mouse fibroblast cell line was cultured with RPMI 1640 and 10% FBS in a culture flask. For obtaining an appropriate cell population, the culture medium was exchanged every three days (3x). After nine days (3x changes), previously sterilized (UV radiation for 15 min)/resized (1.00 cm²), ENs were placed in each well of the 24-well plate. Next, 15,000 to 20,000 cells were used for the seeding process. An equal amount of the culture medium was considered in each well, and plates were incubated (at 37.00 °C and 5.00% CO₂; Memmert, Schwabach, Germany) for the designated period. For assessing the biocompatibility and possible cytotoxicity of ENs, the viability ratios of the seeded cells were evaluated by MTT test at 12, 24, 48, and 72 hr after the cell seeding process. For this purpose, 10.00 µL of reconstituted MTT solution was added to each well containing 100.00 µL of culture medium and 15,000-20,000 seeded cells. After that, the wells were returned to the incubator (37.00 °C and 5.00% CO₂) for 2 hr. Next, 100.00 µL of detergent reagent (equal volume to culture medium) was added to each well. The substrate and background absorbance ratios were recorded by ELISA reader at 570 nm and 690 nm, respectively.

For cell viability calculation, the averages of duplicate sample absorbance ratios were included in the formula as follows:

$$\text{Cytotoxicity \%} = [100 \times (\text{Control} - \text{Sample})] / \text{Control}$$

Statistical analysis. The statistical analyses were performed using SPSS (version 23.00; IBM Corp., Armonk, USA) software. One-way analysis of variance with Tukey post hoc test was used. The *p*-value of less than 0.05 was considered statistically significant. Data values are represented as mean ± SD, and triplicated samples were evaluated for each group and period.

Results

Field emission scanning electron microscopy observations. The nanofibers of Ch/PVA1, an EN with the lowest Ch, represented a rough surface, slight broadening, and irregular fiber orientation. However, increasing Ch percentage could successfully improve the properties mentioned above. Accordingly, by increasing Ch percentage (40.00%-50.00%), the nanofibers were oriented in a proper alignment. They represented smooth surfaces as well as uniform thicknesses.

In contrast, nanofibers' thickness increased to about 1200 nm, and the vast size distribution of fibers was revealed when > 50.00% of Ch was included. Therefore, Ch/PVA5 EN was excluded from the study due to non-nanoscale characteristics. The borax included ENs presented a remarkable cross-link between fibers (Fig. 1).

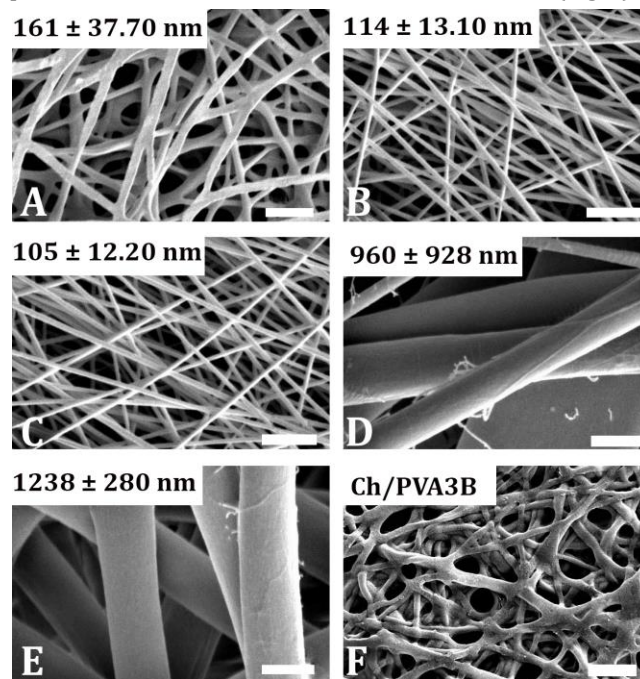


Fig. 1. Field emission scanning electron microscopy images of chitosan/polyvinyl alcohol (Ch/PVA) electrospun nanofibers (ENs). **A)** Ch/PVA1; **B)** Ch/PVA2; **C)** Ch/PVA3; **D)** Ch/PVA4; **E)** Ch/PVA5; **F)** Ch/PVA3 borax included EN, (Scale bars=1 µm).

Weight loss, water absorbability, and structural stability. The weight loss ratio was increased in ENs in a time-dependent manner (Figs. 2A and 2B). ENs weight was maintained based on increasing Ch concentration.

The borax-included ENs exhibited high stability against hydrolysis compared to the non-included ones (Fig. 2C). The results for the water absorbability ratio are presented in Figures 2D-2F. All ENs exhibited significant water absorbability, and the water absorbability was increased by increasing the Ch concentration. Figures 2D and 2E are explaining the time-dependent changes in water absorption trend for borax-included and non-included ENs. Figure 2F represents data to understand better the water absorbability of Ch/PVA3 ENs with and without borax at corresponding periods. The borax-included ENs represent higher water absorbability compared to non-included ones. The Ch/ PVA1 and

Ch/PVA1B ENs were rapidly broken down when immersed in the PBS. Therefore, the results for these ENs are not included in the graphs.

For further investigation, the effect of borax on ENs structural stability, the weight loss test was considered for Ch/PVA3 as an EN without borax and Ch/PVA3B as an EN with borax in different periods using FESEM. The FESEM images are presented in Figure 3. As shown, when the specimen Ch/PVA3 was subjected to a PBS for one day, the EN lost its fibrous structure. Likewise, this phenomenon was observed on the third and seventh days after immersing in PBS. In contrast, the Ch/PVA3B ENs represented surface and shape stability.

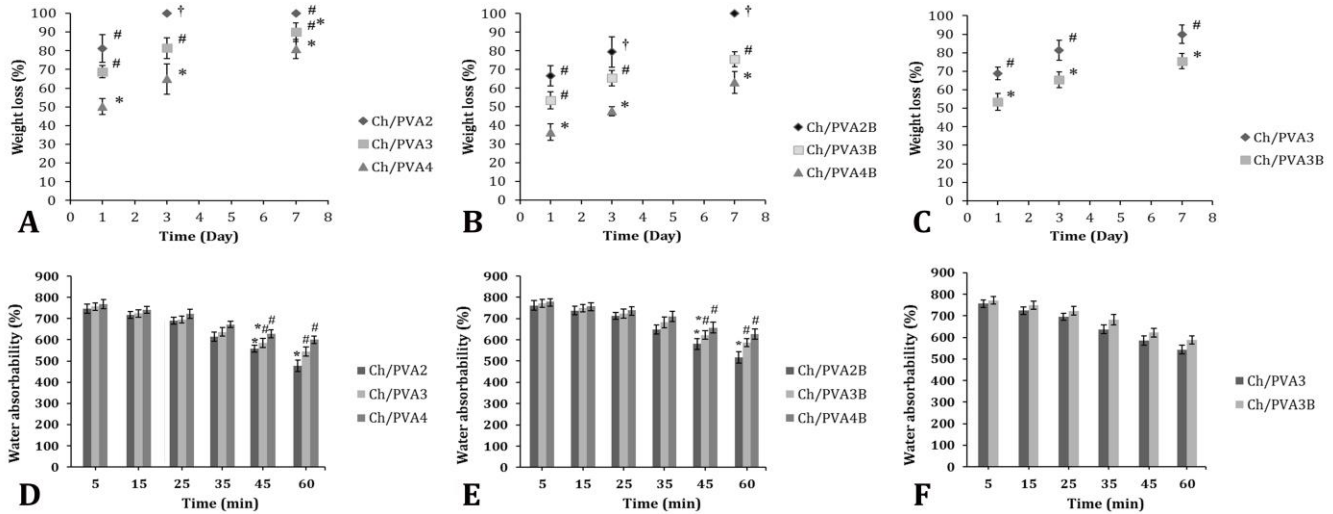


Fig. 2. Weight loss percentages of borax-non-included (A), and borax-included electrospun nanofibers (ENs) (B), at different times are compared. Also, the comparison of weight loss in borax-included and non-included ENs at different periods is presented (C). Furthermore, changes in water absorbability at different periods in non-borax-included (D), borax-included (E), and comparison of water absorbability in borax-included and non-borax-included ENs (Ch/PVA3B and Ch/PVA3, respectively) at different periods are shown (F). Ch/PVA: Chitosan/polyvinyl alcohol; B: Borax.

*#† Different symbols are indicating significant differences at a corresponding time among ENs ($p < 0.05$).

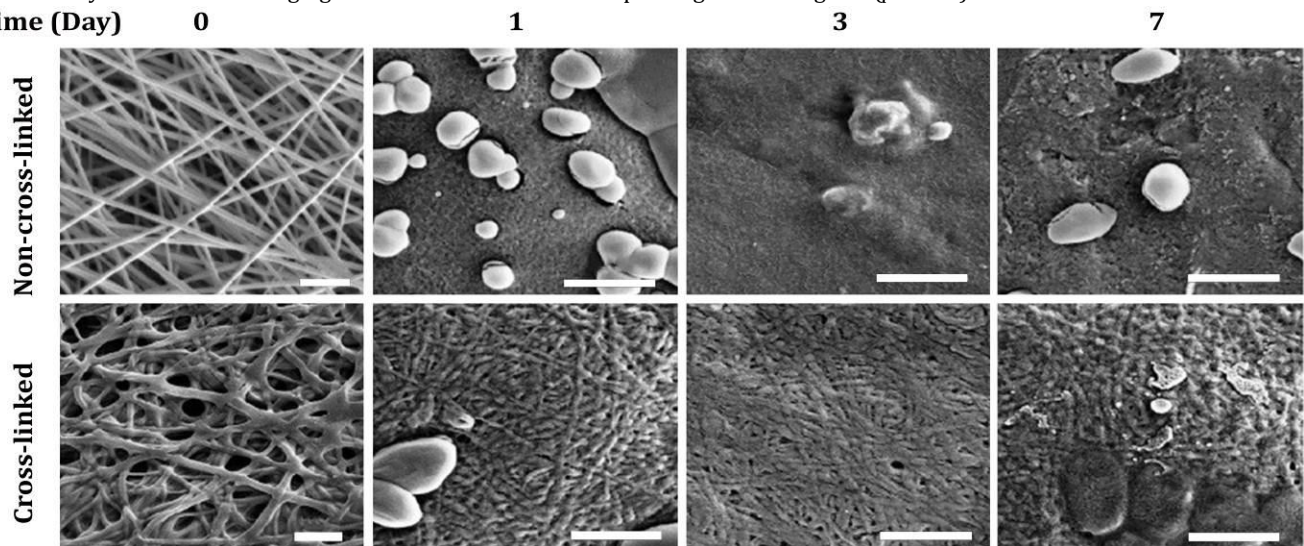


Fig. 3. Field emission scanning electron microscopy of degraded borax-non-included (non-cross-linked) and borax-included (cross-linked) ENs in phosphate-buffered solution at different times. (Scale bars=1 μ m).

Tensile strength test. As a preliminary finding, the tensile strength of borax-included samples with appropriate cross-linkage was significantly higher than non-included ones. Meanwhile, the tensile strength was diminished when Ch was included more than 50.00%. Accordingly, the Ch/PVA4 sample exhibited a weakened tensile strength versus Ch/PVA3 due to nanofibers' non-uniformity (Fig. 4).

MTT assay. The MTT assay represented diminished cell viability 12 hr after seeding in borax-included and non-included ENs. Meanwhile, this situation was compensated time-dependently. Accordingly, the borax-included ENs represented a significant enhancement in cell viability 24 and 48 hr after seeding. Finally, the borax-included ENs represented remarkably higher cell viability compared to non-included ones (Fig. 5).

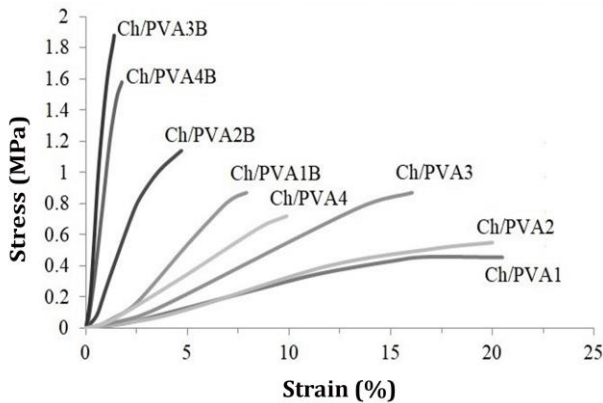


Fig. 4. Stress-strain curves of borax-included (B) and non-included chitosan (Ch)/polyvinyl alcohol (PVA) electrospun nanofibers.

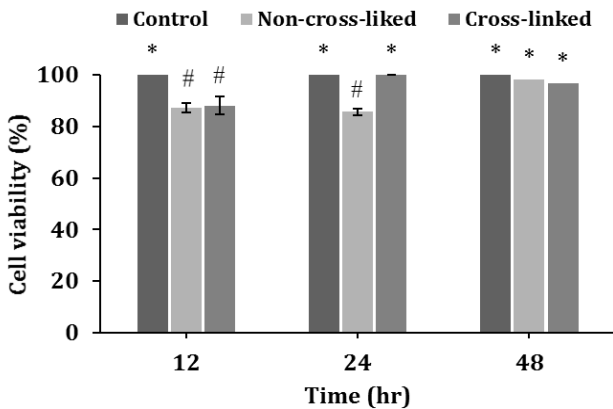


Fig. 5. MTT test for the viability determination of seeded cells on borax-included (cross-linked) and non-included (non-cross-linked) electrospun nanofibers (ENs) at different times. Different symbols are indicating significant differences at a corresponding time among ENs ($p < 0.05$).

Antibacterial test. The results of antibacterial activity are presented in Figure 6. All EN types (borax-included and non-included) inhibited three bacterial species growth. This inhibition was limited to the contact

surface between ENs and the bacteria. In contrast, complete bacterial growth was revealed under sterile gauze in the control group. These findings approved the antibacterial effect of ENs.

Discussion

The structural characteristics, including diameter, orientation, and shape of fibers, are known as the elementary and the most critical factors regarding ENs as a scaffold. The ECM is a natural scaffold containing fibers at a nanoscale diameter. It represents a well-oriented network produced by collagen fibers.³³ Therefore, the production and fabrication of an EN with the same characteristics will enhance its quality and applicability. In the present study, to mimic the produced ENs with natural ECM, different Ch/PVA formulations were used in the ENs fabrication process. Both Ch/PVA2 and Ch/PVA3 ENs represented well-oriented nanofibers with an appropriate diameter and shape compared to other formulations. In a study by Naghavi Alhosseini *et al.*, the Ch and PVA were formulated as Ch 25.00%v/PVA 75.00%v. The ENs from this concentration represented nanofibers with irregular orientation, non-uniform shape, and high fiber diameter (300 - 500 nm).¹⁴ Meanwhile, in the current study, Ch 50.00%v/PVA 50.00%v (Ch/PVA3) resulted in a uniform shape and lower diameter (105 nm). Comparing with others, the Ch/PVA2 and Ch/PVA3 ENs exhibited better uniformity in diameter, shape, and alignment.³⁴⁻³⁹ According to these data, the Ch/PVA2 and Ch/PVA3 ENs represent acceptable characteristics versus other formulations and types and could be considered ENs with higher similarity to ECM.

It is well-known that ECM as a developed tissue provides a microenvironment that its cellular population can migrate, proliferate and differentiate to various cell types freely. Thus, the scaffold, in turn, based on its structure, resistance against hydrolysis, and mechanical strength, should mimic the same situation.⁴⁰ In the above-noted studies, the Ch/PVA ENs were fabricated and used without testing their structural stability in an aqueous environment. Therefore, structural stability remains a primary unknown subject. In line with this issue, the structural stability of ENs was analyzed in the current study. According to our findings, none of the Ch/PVA ENs represented stability in the aqueous environment. To better understand why stability is essential in medication, it should be noted that ENs scaffold designed to mimic the native/physiological ECM. Among different synthetic scaffolds properties, their cross-linkage is known as a factor remarkably affecting the biomechanical characteristics. Indeed, the appropriate/acceptable cross-linking between nanofibers improves the ENs hydrolysis resistance and mechanical strength.²⁵

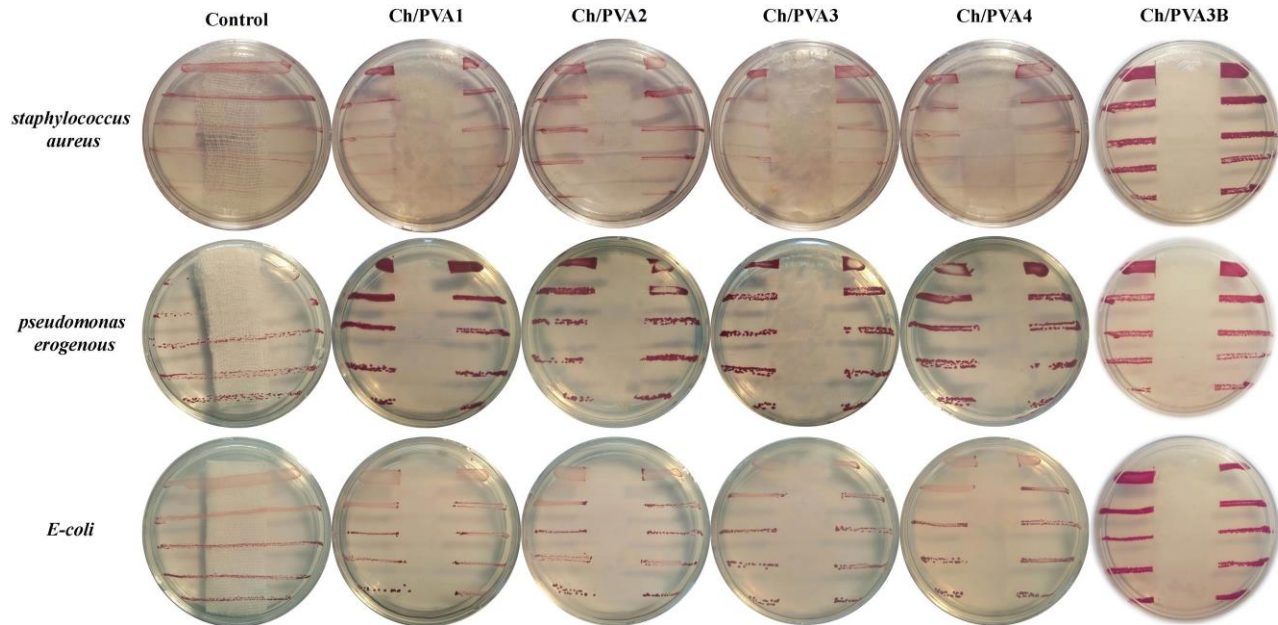


Fig. 6. Anti-bacterial activity of ENs against *S. aureus*, *P. aeruginosa* and *E. coli*. Bacterial growth inhibition exhibits ENs anti-bacterial activity in borax- included and non-included ENs.

Therefore, to obtain appropriate hydrolysis resistance and structural stability in an aqueous environment and improve mechanical strength, borax was included as a cross-linking agent in the ENs formulation in the current study. Based on the acceptable diameter, orientation, and shape of fibers in Ch/PVA2 and Ch/PVA3, these ENs were selected. Next, due to higher hydrolysis resistance of Ch/PVA3 (versus Ch/PVA2) in PBS and minding that the scaffolds are usually considered for long-term aims (> 7 days),⁴¹ the Ch/PVA3 was selected for borax inclusion. FESEM analyses confirmed the cross-linking between the fibers. In this line, cross-linking ENs (borax-included) represented a significant improvement in hydrolysis resistance and biomechanical properties than the non-cross-linking ones (non-borax-included). As it is known well, most ENs are used to transport and improve the tissue-specific cell population after *in vitro* cell or tissue culture. Therefore, the ENs stability in an aqueous environment enhances their applicability in medication systems. Based on our data, borax could induce the cross-linking potential of fibers in ENs. This characteristic could enhance their application in *in vitro* cell culture conditions and tissue after possible surgical implantation. In addition to hydrolysis resistance, the scaffolds should contain individual formulations to absorb/maintain necessary fluids for cellular content appropriately.⁴² According to our findings, approximately all ENs (with different formulations) represented high water absorbability. However, the borax-included ENs expressed higher water absorbability versus non-included ones. Indeed, as mentioned above, the scaffolds' cellular contents need to

be seeded in an environment with high fluidity to exert better viability, proliferation, and physiological interactions.⁴³ Thus, borax was found to provoke structural stability and water absorbability, simultaneously with increasing the ENs hydrolysis resistance. As a preliminary conclusion, increased hydrolysis stability and water absorbability candidate the borax-included ENs as an appropriate scaffold in tissue engineering. A higher live cell population (marked with MTT) approved this conclusion. Also, the applicability of scaffolds by operators (usually surgeons) in different situations and sites is one of the essential aspects of scaffold design. In this study, borax-included ENs represented proper handling and adequate mechanical strength compared to non-included ones.

Microbial contamination is one of the critical problems in the wound healing process.⁴⁴ Essential bacteria causing wound infection are *Staphylococcus* species, especially *S. aureus*, *P. aeruginosa*, and *E. coli*.^{45,46} Moreover, in tissue engineering, the possibility of contamination increases due to the cell seeding process on the scaffold. In this line, in several studies, nanoparticles (especially silver) have been used to enhance the antibacterial properties of ENs.^{47,48} For instance, Abdelgawad *et al.* have loaded silver nanoparticles to Ch/PVA ENs to improve their antibacterial activity against *E. coli*.³⁴ Although silver nanoparticles are known for their antibacterial properties, these nanoparticles can induce mitochondrial and DNA damage in somatic cells or corresponding seeded cells population.⁴⁹ In this study, based on antibacterial and MTT tests, the ENs exhibited antibacterial activity against Gram-

positive and Gram-negative bacteria and, at the same time, did not affect the cellular viability. Therefore, the Ch/PVA ENs can exert an appropriate antibacterial effect in the sole form without other nano-coating processes.

According to our findings, the EN containing Ch50.00%v/PVA50.00%v exerts appropriate morphological and biomechanical properties compared to other ENs. Furthermore, borax-included ENs were improved regarding biomechanical and biocompatibility properties.

In conclusion, according to the results of fluid absorbance, hydrolysis resistance, structural stability in the aquatic environment, tensile strength, and antibacterial properties of ENs and based on cell viability analysis outcome, borax-included ENs can be considered as an appropriate scaffold in tissue engineering. However, *in vivo* trials are needed to clear their side effects and advantages.

Acknowledgments

This study was supported by the Vice-Chancellor for Research of Urmia University, Urmia, Iran.

Conflict of interest

The authors declare that there is no conflict of interest regarding the publication of this paper.

References

- Jiang T, Carbone EJ, Lo KW-H, et al. Electrospinning of polymer nanofibers for tissue regeneration. *Prog Polym Sci* 2015; 46:1-24.
- Bai H, Wang D, Delattre B, et al. Biomimetic gradient scaffold from ice-templating for self-seeding of cells with capillary effect. *Acta Biomater* 2015; 20:113-119.
- Günther MI, Weidner N, Müller R, et al. Cell-seeded alginate hydrogel scaffolds promote directed linear axonal regeneration in the injured rat spinal cord. *Acta Biomater* 2015; 27:140-150.
- Vocetkova K, Buzgo M, Sovkova V, et al. Nanofibrous polycaprolactone scaffolds with adhered platelets stimulate proliferation of skin cells. *Cell Prolif* 2016; 49(5):568-578.
- Bean AC, Tuan RS. Fiber diameter and seeding density influence chondrogenic differentiation of mesenchymal stem cells seeded on electrospun poly (ϵ -caprolactone) scaffolds. *Biomed Mater* 2015; 10(1):015018. doi: 10.1088/1748-6041/10/1/015018.
- Chen JP, Chang GY, Chen JK. Electrospun collagen/chitosan nanofibrous membrane as wound dressing. *Colloids Surf A Physicochem Eng Asp* 2008; 313-314:183-188.
- Gomes SR, Rodrigues G, Martins GG, et al. *In vitro* and *in vivo* evaluation of electrospun nanofibers of PCL, chitosan and gelatin: a comparative study. *Mater Sci Eng C Mater Biol Appl*. 2015; 46:348-358.
- Rieger KA, Birch NP, Schiffman JD. Electrospinning chitosan/poly (ethylene oxide) solutions with essential oils: Correlating solution rheology to nanofiber formation. *Carbohydr Polym* 2016; 139:131-138.
- Zhang Y, Venugopal JR, El-Turki A, et al. Electrospun biomimetic nanocomposite nanofibers of hydroxyl-apatite/chitosan for bone tissue engineering. *Biomaterials* 2008; 29(32):4314-4322.
- Kun M, Chan C, Ramakrishna S. Textile-based scaffolds for tissue engineering, In: Rajendran s. (Ed.) *Advanced textiles for wound care*. Cambridge, UK; Woodhead Publishing 2019: 329-362.
- Younes I, Rinaudo M. Chitin and chitosan preparation from marine sources. Structure, properties and applications. *Mar Drugs* 2015; 13(3):1133-1174.
- Costa-Pinto AR, Martins AM, Castelhana-Carlos MJ, et al. *In vitro* degradation and *in vivo* biocompatibility of chitosan-poly(butylene succinate) fiber mesh scaffolds. *J Bioact Compat Polym* 2014; 29(2):137-151.
- Muxika A, Etxaberria AE, Uranga J, et al. Chitosan as a bioactive polymer: Processing, properties and applications. *Int J Biol Macromol* 2017; 105: 1358-1368.
- Naghavi Alhosseini S, Moztarzadeh F, Mozafari M, et al. Synthesis and characterization of electrospun polyvinyl alcohol nanofibrous scaffolds modified by blending with chitosan for neural tissue engineering. *Int J Nanomedicine* 2012; 7: 25-34.
- Dhandayuthapani B, Krishnan UM, Sethuraman S. Fabrication and characterization of chitosan-gelatin blend nanofibers for skin tissue engineering. *J Biomed Mater Res B Appl Biomater* 2010; 94(1):264-272.
- Subramanian A, Vu D, Larsen GF, et al. Preparation and evaluation of the electrospun chitosan/PEO fibers for potential applications in cartilage tissue engineering. *J Biomater Sci Polym Ed* 2005; 16(7):861-873.
- Xu CY, Inai R, Kotaki M, et al. Aligned biodegradable nanofibrous structure: a potential scaffold for blood vessel engineering. *Biomaterials* 2004; 25(5):877-886.
- Dvir T, Timko BP, Kohane DS, et al. Nanotechnological strategies for engineering complex tissues. *Nat Nanotechnol* 2011; 6:13-22.
- Bhardwaj N, Kundu SC. Electrospinning: a fascinating fiber fabrication technique. *Biotechnol Adv* 2010; 28(3):325-347.
- Jalaja K, Naskar D, Kundu SC, et al. Potential of electrospun core-shell structured gelatin-chitosan nanofibers for biomedical applications. *Carbohydr Polym* 2015; 136:1098-1107.
- Jia YT, Gong J, Gu XH, et al. Fabrication and characterization of poly (vinyl alcohol)/chitosan blend nanofibers produced by electrospinning method. *Carbohydr Polym* 2007; 67(3):403-409.

22. Ji Y, Ghosh K, Li B, et al. Dual-syringe reactive electrospinning of cross-linked hyaluronic acid hydrogel nanofibers for tissue engineering applications. *Macromol Biosci* 2006; 6(10):811-817.
23. Ko JH, Yin HY, An J, et al. Characterization of cross-linked gelatin nanofibers through electrospinning. *Macromol Res* 2010; 18:137-143.
24. Panzavolta S, Gioffrè M, Focarete ML, et al. Electrospun gelatin nanofibers: optimization of genipin cross-linking to preserve fiber morphology after exposure to water. *Acta Biomater* 2011; 7(4):1702-1709.
25. Schiffman JD, Schauer CL. Cross-linking chitosan nanofibers. *Biomacromolecules* 2007; 8(2):594-601.
26. Sarika PR, Cinthya K, Jayakrishnan A, et al. Modified gum arabic cross-linked gelatin scaffold for biomedical applications. *Mater Sci Eng C Mater Biol Appl* 2014; 43:272-279.
27. Sreedhar B, Sairam M, Chattopadhyay DK, et al. Thermal, mechanical, and surface characterization of starch-poly(vinyl alcohol) blends and borax-cross-linked films. *J Appl Polym Sci* 2005; 96(4):1313-1322.
28. Balakrishnan B, Jayakrishnan A. Self-cross-linking biopolymers as injectable in situ forming biodegradable scaffolds. *Biomaterials* 2005; 26(18):3941-3951.
29. Sangsanoh P, Supaphol P. Stability improvement of electrospun chitosan nanofibrous membranes in neutral or weak basic aqueous solutions. *Biomacromolecules* 2006; 7(10):2710-2714.
30. Bhattarai N, Edmondson D, Veiseh O, et al. Electrospun chitosan-based nanofibers and their cellular compatibility. *Biomaterials* 2005; 26(31):6176-6184.
31. Karuppuswamy P, Venugopal JR, Navaneethan B, et al. Polycaprolactone nanofibers for the controlled release of tetracycline hydrochloride. *Mater Lett* 2015; 141:180-186.
32. Liu X, Lin T, Fang J, et al. *In vivo* wound healing and antibacterial performances of electrospun nanofibre membranes. *J Biomed Mater Res A* 2010; 94(2):499-508.
33. Davis SC, Ricotti C, Cazzaniga A, et al. Microscopic and physiologic evidence for biofilm-associated wound colonization *in vivo*. *Wound Repair Regen* 2008; 16(1):23-29.
34. Abdelgawad AM, Hudson SM, Rojas OJ. Antimicrobial wound dressing nanofiber mats from multicomponent (chitosan/silver-NPs/polyvinyl alcohol) systems. *Carbohydr Polym* 2014; 100:166-178.
35. Charernsriwilaiwat N, Opanasopit P, Rojanarata T, et al. Preparation and characterization of chitosan-hydroxy benzotriazole/polyvinyl alcohol blend nanofibers by the electrospinning technique. *Carbohydr Polym* 2010; 81(3):675-680.
36. Charernsriwilaiwat N, Rojanarata T, Ngawhirunpat T, et al. Electrospun chitosan/polyvinyl alcohol nanofibre mats for wound healing. *Int Wound J* 2014; 11(2): 215-222.
37. Hang AT, Tae B, Park JS. Non-woven mats of poly (vinyl alcohol)/chitosan blends containing silver nanoparticles: Fabrication and characterization. *Carbohydr Polym* 2010; 82(2):472-479.
38. Park JH, Lee HW, Chae DK, et al. Electrospinning and characterization of poly (vinyl alcohol)/chitosan oligosaccharide/clay nanocomposite nanofibers in aqueous solutions. *Colloid Polym Sci* 2009; 287:943-950.
39. Yan E, Fan S, Li X, et al. Electrospun polyvinyl alcohol/chitosan composite nanofibers involving Au nanoparticles and their *in vitro* release properties. *Mater Sci Eng C Mater Biol Appl* 2013; 33(1): 461-465.
40. Vernekar VN, James R, Smith KJ, et al. Nanotechnology applications in stem cell science for regenerative engineering. *J Nanosci Nanotechnol* 2016; 16(9): 8953-8965.
41. Velnar T, Bailey T, Smrkolj V. The wound healing process: an overview of the cellular and molecular mechanisms. *J Int Med Res* 2009; 37(5):1528-1542.
42. Boateng JS, Matthews KH, Stevens HN, et al. Wound healing dressings and drug delivery systems: a review. *J Pharm Sci* 2008; 97(8):2892-2923.
43. Kerch G. Polymer hydration and stiffness at biointerfaces and related cellular processes. *Nano medicine* 2018; 14(1):13-25.
44. Mirjalili A, Parmoor E, Bidhendi SM, et al. Microbial contamination of cell cultures: a 2 years study. *Biologicals* 2005; 33(2):81-85.
45. Kadler K. Matrix loading: assembly of extracellular matrix collagen fibrils during embryogenesis. *Birth Defects Res C Embryo Today: Reviews* 2004; 72(1): 1-11.
46. Bjarnsholt T, Kirketerp-Møller K, Jensen PØ, et al. Why chronic wounds will not heal: a novel hypothesis. *Wound Repair Regen* 2008; 16(1):2-10.
47. Kohsari I, Shariatinia Z, Pourmortazavi SM. Antibacterial electrospun chitosan--polyethylene oxide nanocomposite mats containing bioactive silver nanoparticles. *Carbohydr Polym* 2016; 140:287-298.
48. Wang X, Cheng F, Gao J, et al. Antibacterial wound dressing from chitosan/polyethylene oxide nanofibers mats embedded with silver nanoparticles. *J Biomater Appl* 2015; 29(8):1086-1095.
49. AshaRani PV, Low Kah Mun G, Hande MP, et al. Cytotoxicity and genotoxicity of silver nanoparticles in human cells. *ACS Nano* 2009; 3(2):279-290.